Table of Contents

Supplementary methods

Method S1. Type I collagen coating.

To support stromal cell adhesion on polyacrylamide hydrogel scaffolds, type I collagen extracted from rat tails was covalently immobilized on the pore surface using Sulfo-SANPAH conjugate chemistry. Sterilized scaffolds were washed in a sterile conjugate buffer solution (20 mM Na_2HPO_4, 0.15 M NaCl at a pH of 7-9) three times and allowed to stabilize for 30 minutes. Roughly 10 mg Sulfo-SANPAH was dissolved in 500 µL dimethyl sulfoxide (DMSO) and diluted in 50 mL of conjugate buffer. This amount of Sulfo-SANPAH is suitable for around 250 scaffolds. Scaffolds were soaked in Sulfo-SANPAH solution and then centrifuged for 10 minutes at 1500 RPM in a centrifuge. Scaffolds were kept in solution for 6 hours at 4 °C with gentle shaking and protected from light with aluminum foil. Scaffolds were then washed 5 times with conjugate buffer to remove excess Sulfo-SANPAH. A working collagen solution was made by diluting sterile collagen solution (2.6 mg/mL) 1:1 with cold sterile filtered 1 mM HCl. Scaffolds were suspended in working collagen solution, placed in a petri dish over ice in a single layer, and exposed to a 15-Watt UV light source for 15 minutes to activate a protected functional group in the conjugate chemistry. Scaffolds were removed from petri dishes and placed into fresh working collagen solution followed by overnight incubation at 4 °C with gentle shaking. The next day, scaffolds were washed 3 times with ice cold, sterile 1 mM HCl followed by washing in sterile PBS. Collagen coated scaffolds were stored at 4 °C in sterile PBS.

Method S2. Multilineage differentiation of human BMSCs.

Prior to osteogenic and adipogenic differentiation, hBMSCs were cultured to 80-90% confluency. Growth media was replaced with differentiation for two weeks, changed every 3 days. Osteogenic differentiation media was composed of αMEM was supplemented with 10% FBS, 1% penicillin-streptomycin, 100 nM dexamethasone, 200 µM ascorbic acid-2-phosphate, and 10 mM glycerol 2-phosphate. Adipogenic differentiation media was composed of αMEM was supplemented with 10% FBS, 1% penicillin-streptomycin, 1 µM dexamethasone, 500 µM 3-isobutyl-1-methylxanthine, and 100 µM indomethacin. For chondrogenic differentiation, cell pellets were formed by centrifuging 250,000 hBMSCs at 1500 RPM for 5 mi in 15 mL conical tubes. Chondrogenic differentiation media was added to the tubes without disrupting the pellet and changed every 3 days for 2 weeks. Conical tubes were returned to the incubator with loosened caps to allow for gas exchange. Chondrogenic differentiation media was composed of serum free Dulbecco's Modified Eagle's Medium (DMEM) supplemented with 1% penicillin-streptomycin, 100 nM dexamethasone, 200 µM ascorbic acid-2-phosphate, 10 ng/mL TGF-β, 1% ITS-premix, and 1 mM sodium pyruvate. Chondrogenic differentiation was confirmed via Safranin O staining.

Method S3. Histological staining.

Frozen tissue sections were fixed with 10% neutral buffered formalin for 10 minutes. After washing with DI water, sides were transferred to hematoxylin for 30 seconds. Slides were then

washed with DI water until dye was no longer present in the effluent and then transferred to eosin Y for 45 seconds. For trichrome staining, frozen tissue sections were fixed with 10% neutral buffered formalin for 10 minutes. After washing with DI water, slides were left in Bouin's fluid overnight at room temperature. The following day slides were washed with DI water until the tissue was colorless. Slides were transferred to Weigert's hematoxylin for 5 minutes followed by thorough rinsing in DI water. Rinsed slides were then placed in Biebrich scarlet-acid fuchsin for 15 minutes and then washed in DI water. Stained slides were transferred to phosphomolybdic/ phosphotungstic acid for 12 minutes before immediate transfer into aniline blue stain for 7 minutes. Slides were then rinsed in DI water before transferring to 1% acetic acid for 5 minutes. Slides were serially dehydrated in 70, 85, and 100% ethanol before xylene. Samples were mounted in Shandon-Mount covered with a glass cover slide. Images were taken with a color camera on an EVOS FL Auto microscope.

Supplementary figures

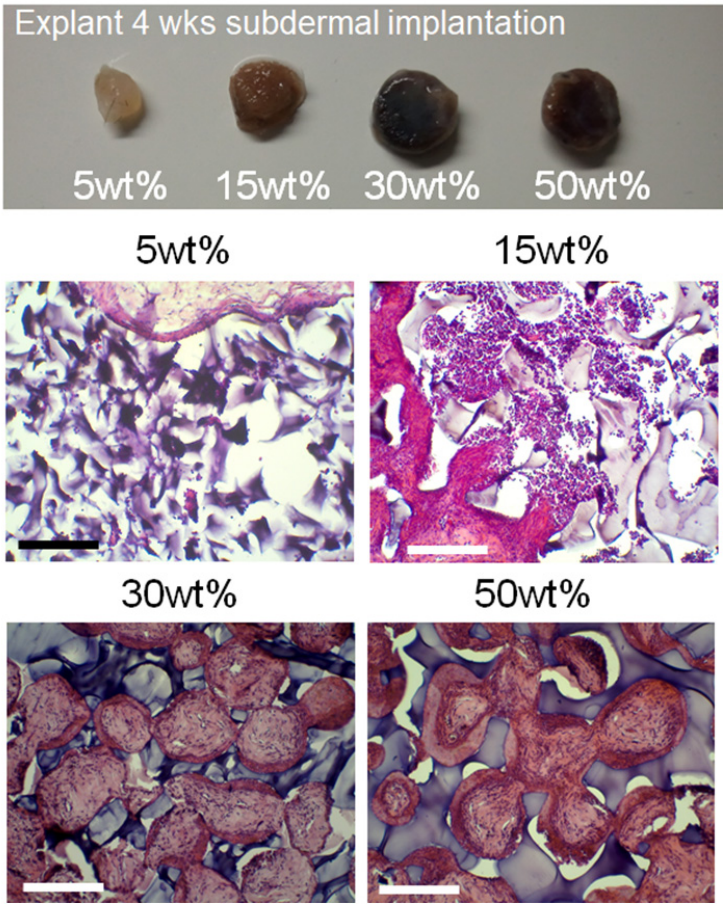

Fig. S1. Inverted colloidal crystal (ICC) polyacrylamide (PAA) hydrogel scaffolds with four different polymer concentrations. Representative gross images of scaffolds after 4 weeks

implantation, and hematoxylin and eosin stained images from 2 independent experiments. Scale bar 200 μm.

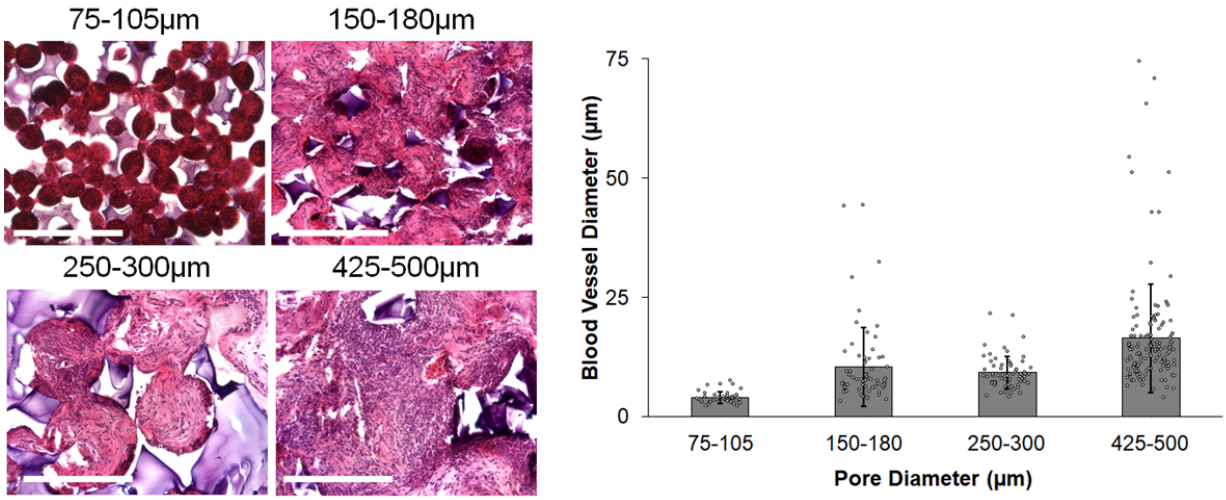

Fig. S2. PAA ICC scaffold with four different pore sizes. Hematoxylin and eosin staining of 30 wt% PAA scaffolds fabricated with different bead sizes. Scaffolds were implanted for 4 weeks. Increasing pore size, resulted in larger vascular diameter (n=2, independent scaffolds, 4 images in each scaffold in which 5-10 vessel measurement) Data are mean ± s.d., Scale bar 250 μm.

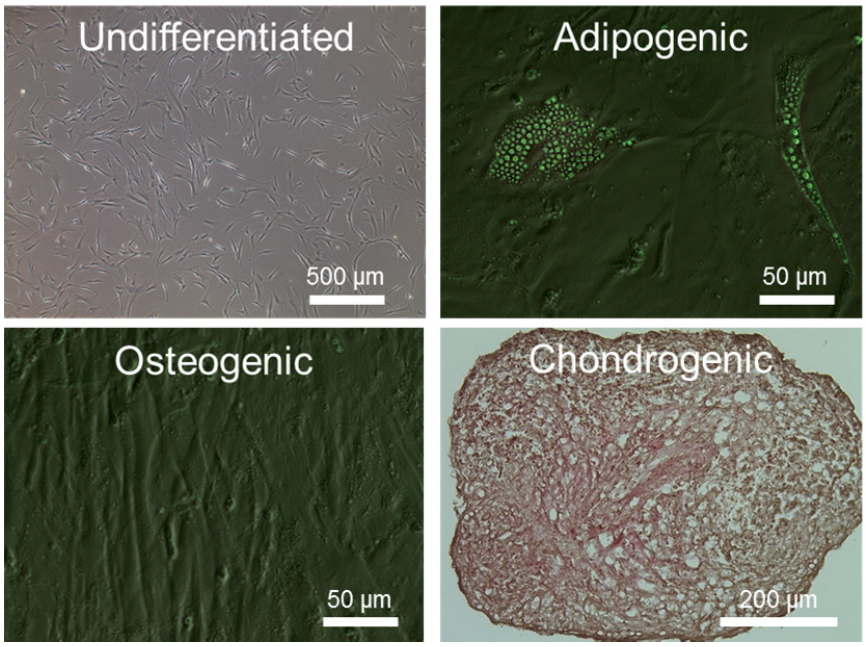

Fig. S3. Human bone marrow stromal cell (hBMSC) multilineage potential. hBMSCs isolated from human bone marrow aspirate have capability to differentiate into adipogenic,

osteogenic, and chondrogenic lineage. Undifferentiated, adipogenic, and osteogenic images are representative brightfield images displaying changes to morphology. Chondrogenic image was taken following Safranin O staining for proteoglycans.

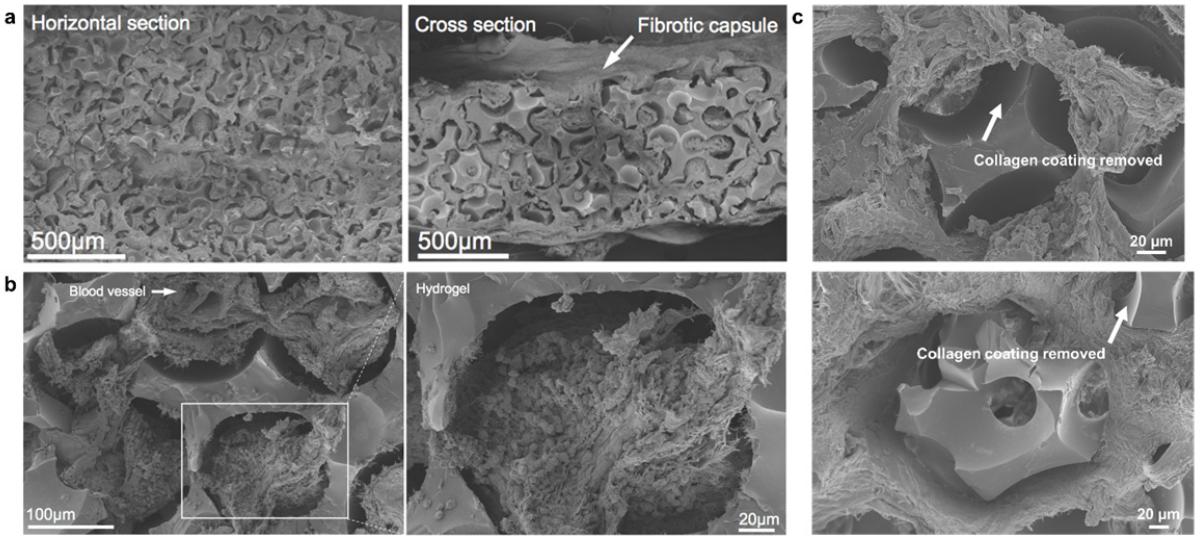

Fig. S4. Scanning electron microscope images of complete tissue infiltration into PAA ICC hydrogel scaffolds. a, Complete tissue infiltration with minimal fibrotic encapsulation of the PAA scaffold. **b**, Vascularization and recruitment of immune cells. **c**, Initial collagen coating removed from acrylamide surface.

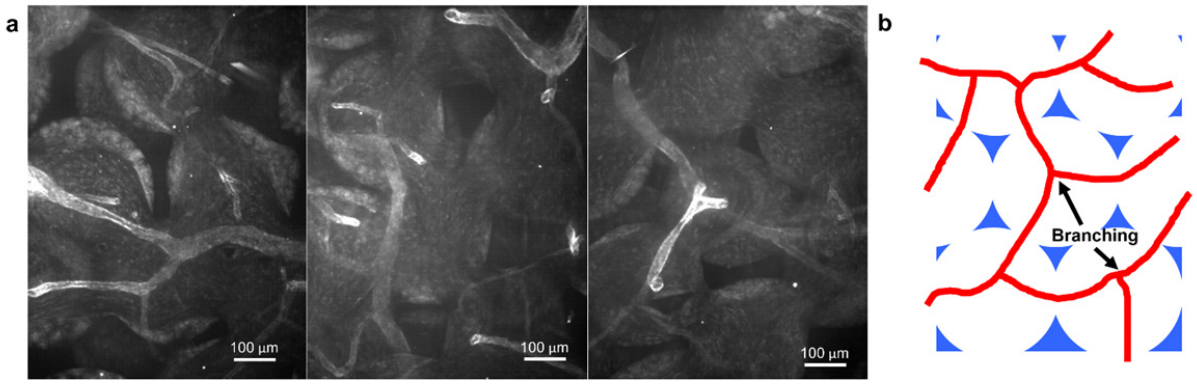

Fig. S5. Branched vascular morphology through interconnecting pores in the ICC scaffold. **a**, Representative immunohistostaining (IHS) of mCD31 through the scaffold. Blood vessels have a branched morphology. **b**, Vascular branching only occurred in the scaffold pores and not at interconnecting junction indicating the vasculature is directed by the biomaterial geometry.

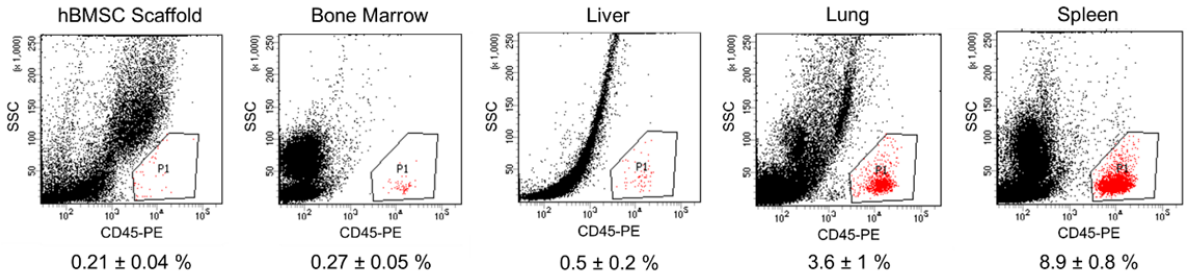

Fig. S6. Flow cytometry plots of hPBMC migration across various tissue. (n=3, independent mice).

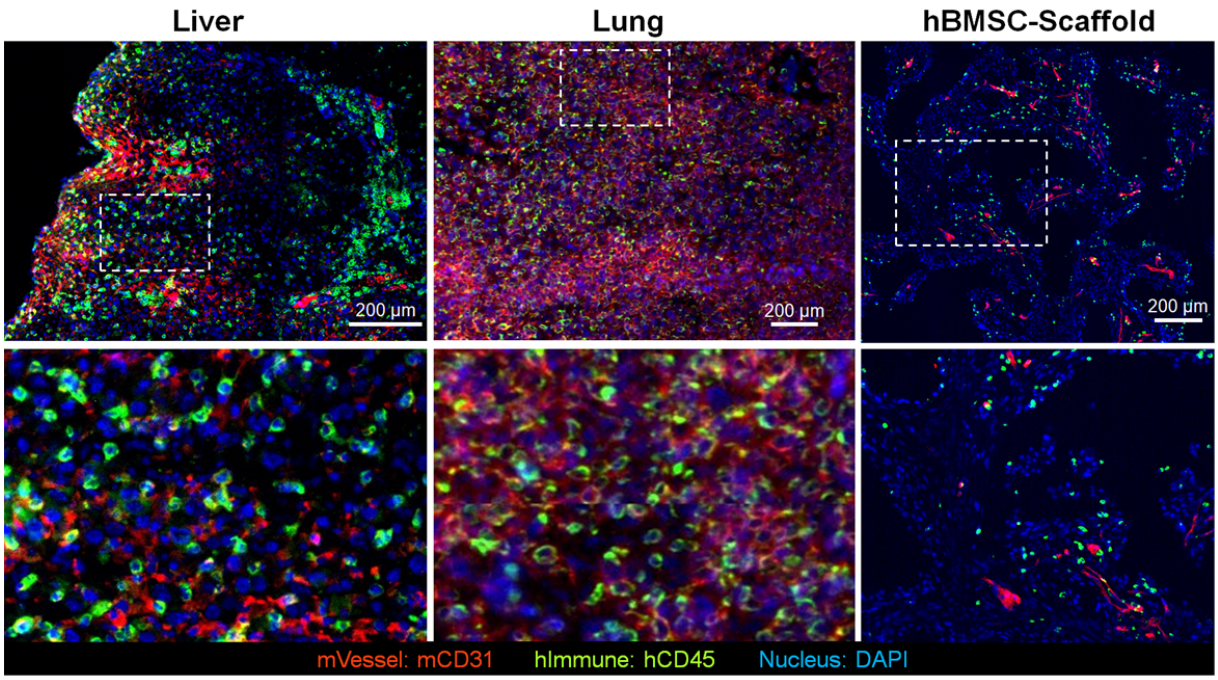

Fig. S7. Distribution of hCD45 cells in primary mice liver, lung, and implanted hBMSC-scaffold 6 weeks after hPBMC injection. IHS shows more human immune cells in native mouse tissues than hBMSC-scaffolds. Immune cells in the scaffold remain largely as single cells. The similar results were confirmed from three independent liver, lung and caffolds characterization.

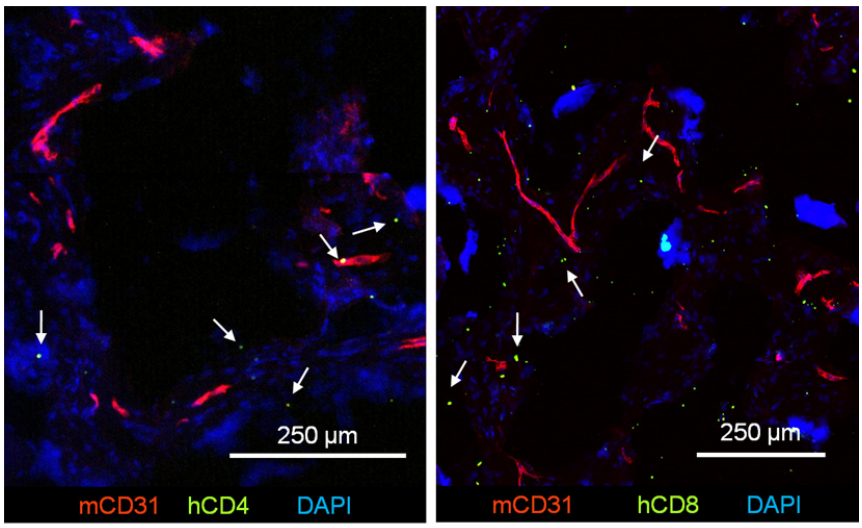

Fig. S8. Human CD4 and CD8 IHS 6 weeks after hPBMC injection. Human CD4 and CD8 cells in hBMSC scaffolds. The similar results were confirmed from three independent scaffolds characterization.

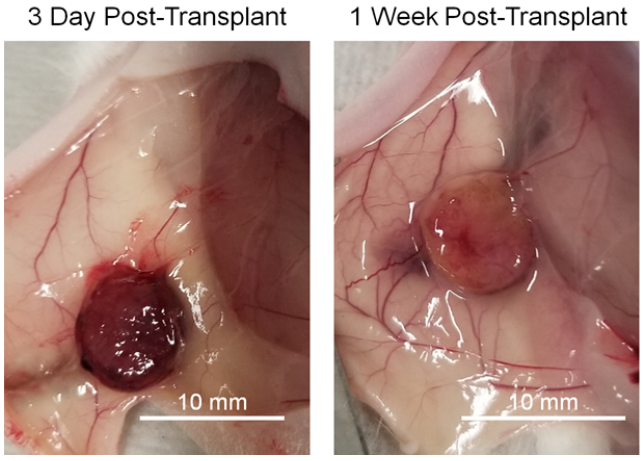

Fig. S9. Large blood vessel recruitment to the transplanted scaffold after 3 and 7 days in secondary mice. Two independent scaffolds were characterized at day 3 and 7 transplantation. Increased large vessel recruitment was observed at day 7. This experiment was performed one time.

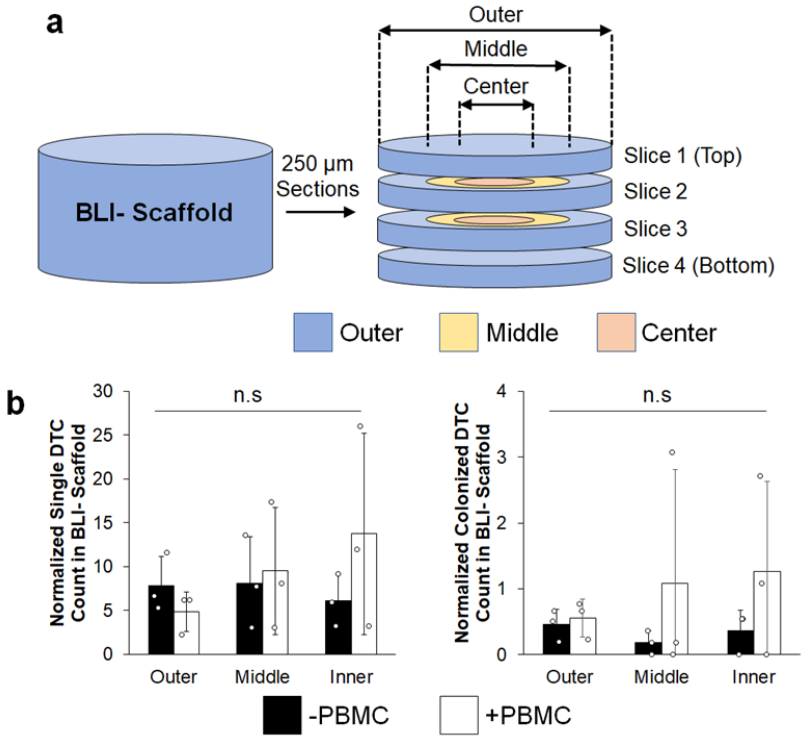

Fig. S10. Spatial dissection of DTCs in BLI- scaffolds. a, Schematic of BLI- scaffold processing and region designation. **b**, Normalized distribution of single and colonized DTCs in each region. (n=3, intendent scaffolds) Data are mean ± s.d. Not significant, P-value > 0.05 via two-sided student t-test.

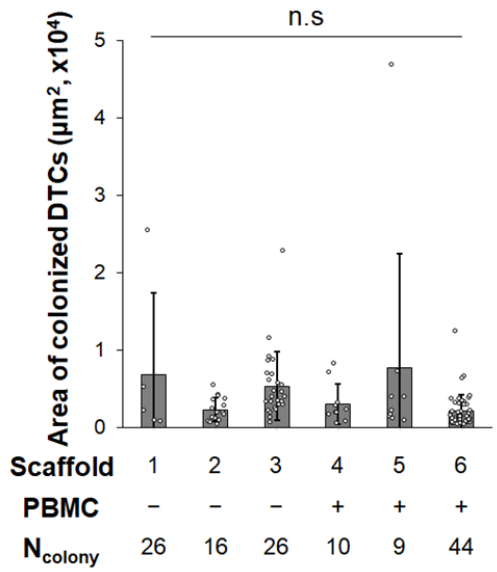

Fig. S11. Colonized DTC size measurements from BLI- scaffolds via whole tissue analysis. Data are mean ± s.d. Not significant, P > 0.05 via two-sided student t-test.

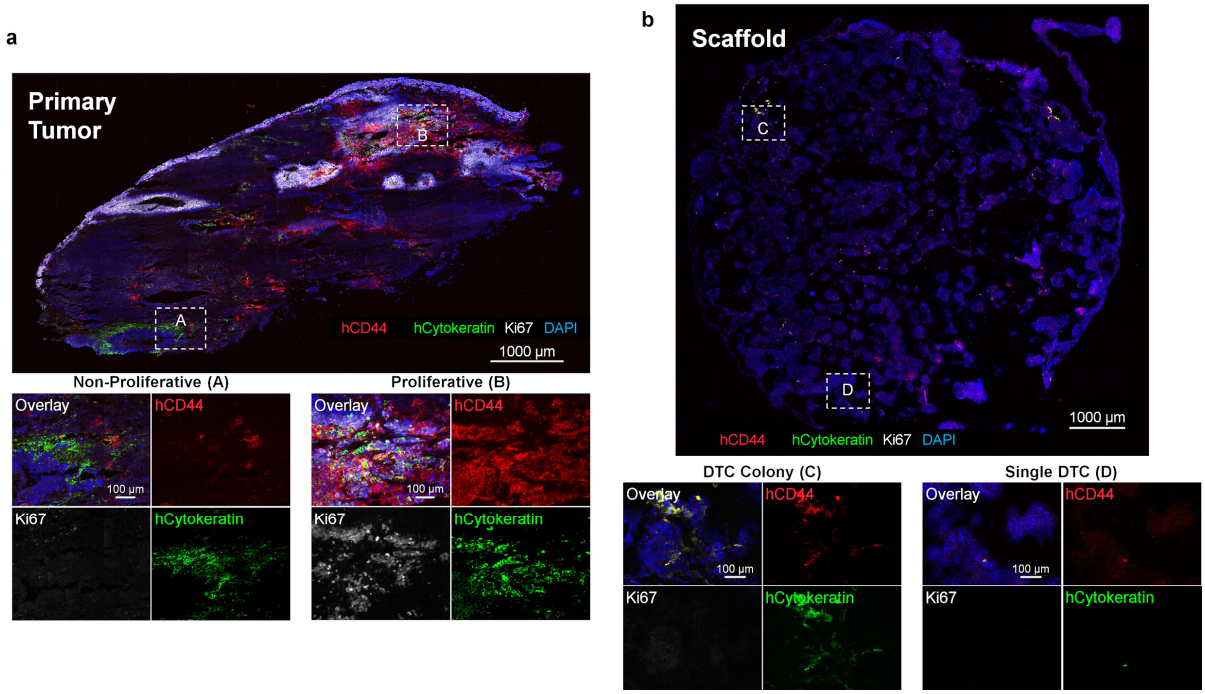

Fig. S12. IHS of Ki67, hCD44 and hCytokeratin in a primary tumor and an implanted hBMSC-scaffold. a, Human CD44 and human cytokeratin do not have high overlap in primary tumor. Proliferative regions of the primary tumor had higher overlap than non-proliferative regions. **b**, Most single and colonized DTCs had overlapping human CD44 and human cytokeratin. Three independent primary tumors and scaffolds were characterized.

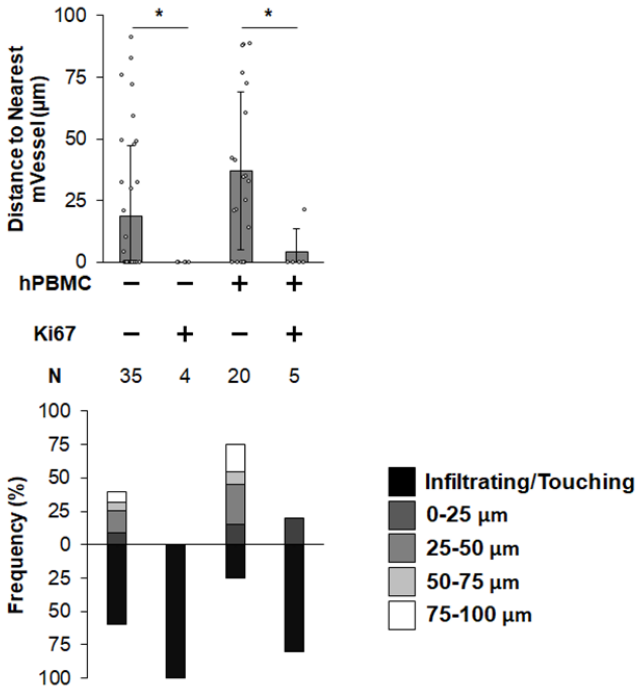

Fig. S13. Correlation between tumor infiltrating vessels and proliferative tumor colonies. Proliferative tumor colonies were always within 25 µm of mouse blood vessel. Data are mean ± s.d. * $P < 0.05$ via two-sided student t-test.

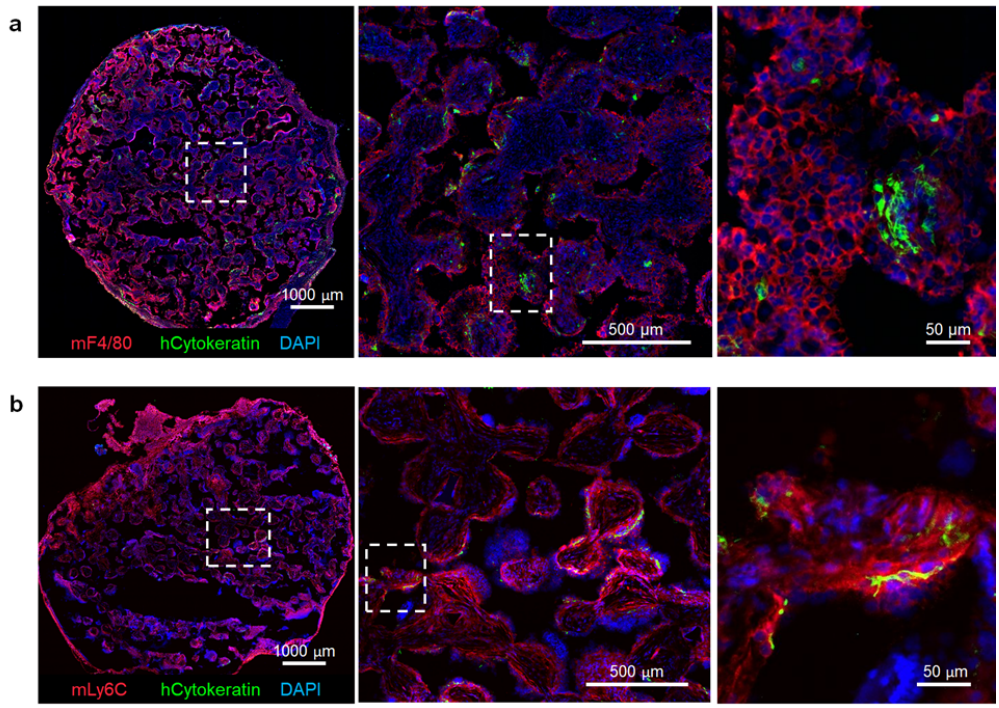

Fig. S14. IHS of mouse F4/80 and Ly6C in hBMSC-scaffold. **a**, Representative IHS images of mF4/80 and **b**, mLy6C staining in disseminated tumor microenvironment from 3 independently characterized scaffolds. Widespread staining made quantification difficult and non-conclusive.

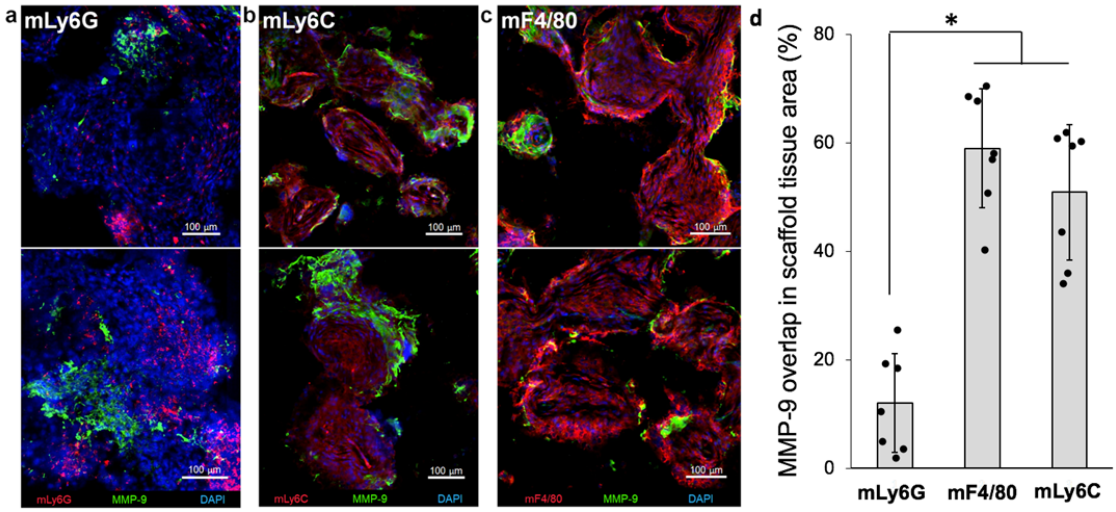

Fig. S15. IHS of MMP-9 in hBMSC-scaffolds. Representative IHS images of **a**, mLy6G, **b**, mLy6C, and **c**, mF4/80 staining in scaffold microenvironment from 3 independent scaffolds. High amounts of MMP-9 at the biomaterial scaffold interface. **d**, Quantification of MMP-9 source reveals mF4/80 and mLy6C cells are main producers. (n=3, independent scaffolds) Data are mean ± s.d. * $P < 0.05$ via two-sided student t-test.

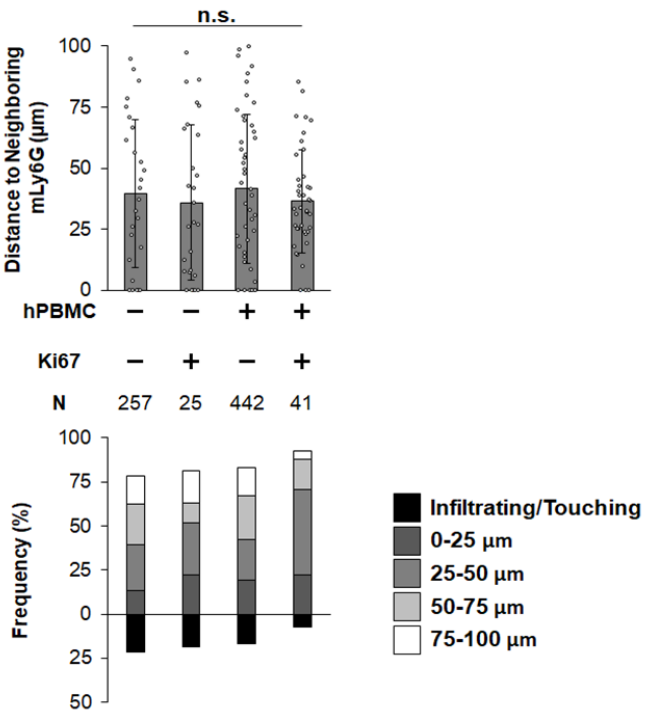

Fig. S16. Correlation between mLy6G and proliferative tumor colonies. No change in local mLy6G cell distribution between proliferative and non-proliferative tumor colonies. Addition of hPBMCs did not influence distribution. Characterization was not performed on singular DTCs since all cells were non-proliferative. Data are mean ± s.d. Not significant, $P > 0.05$ via two-sided student t-test.

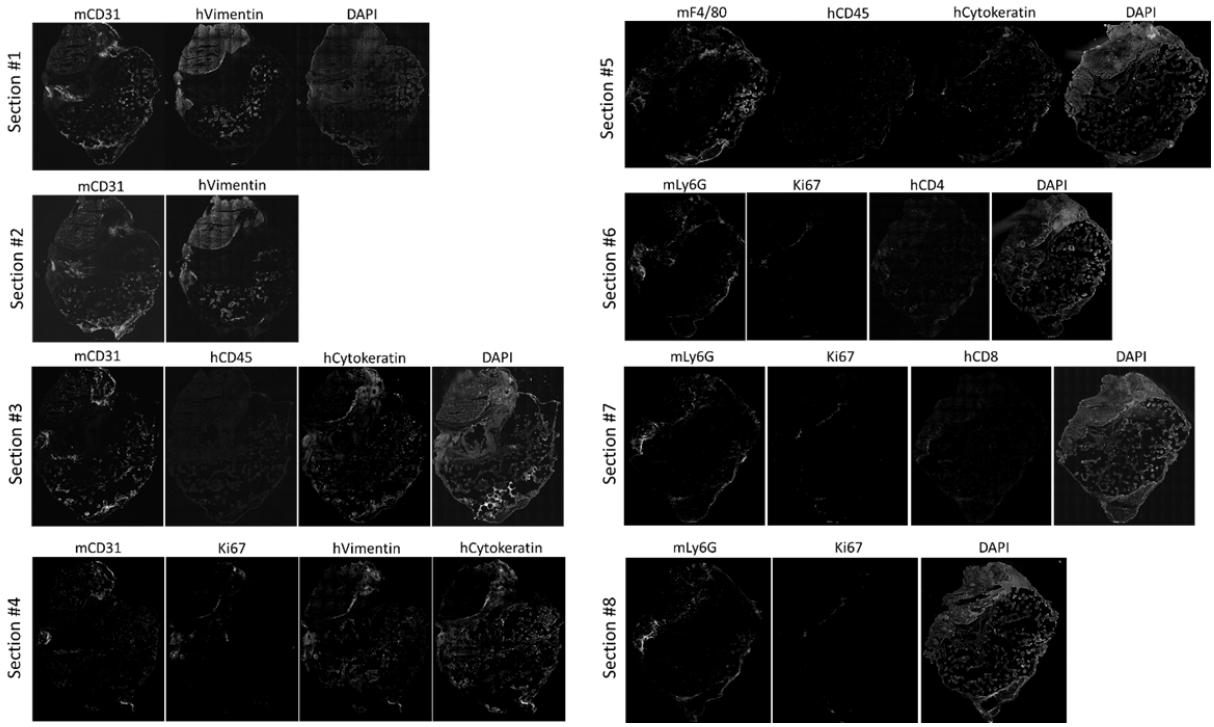

Fig. S17. IHS of eight consecutive overt metastasis slices with different antibody staining. Ten different antibody staining was conducted in this overt metastatic scaffold. Defined set of antibody staining was conducted in two independent overt metastatic scaffolds in Fig. S20.

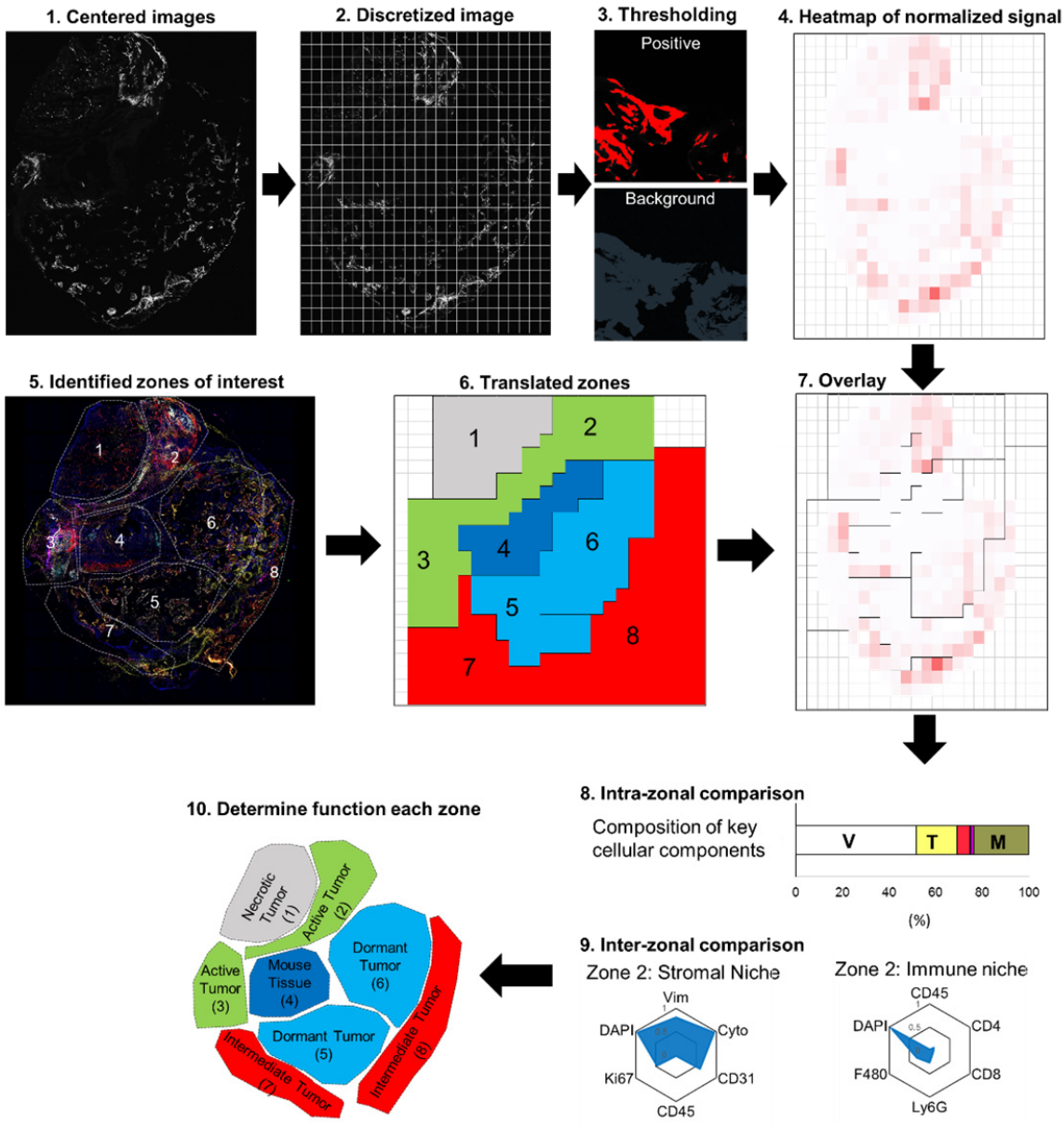

Fig. S18. Active tumor microenvironment imaging analysis pipeline.

1) Images were centered and canvas size equalized.
2) Scaffold images discretized into 24x24 grid of subimages.
3) For each antibody positive signal separated from background noise. Total tissue area was calculated by increasing background to include autofluorescent tissue.
4) Positive signal from each subimage was normalized to total tissue area and displayed as a heatmap.
5) Visual inspection of images revealed 8 zones that housed unique features.
6) Manually determined zones of interest translated to 24x24 grid.

7) The 8 translated zones were overlaid on images with normalized signal. Normalized signal was recalculated for each of the 8 zones.
8) Intra-zonal composition was performed by dividing the positive pixels for each stain and dividing by the summation of all positive pixels from all staining except Ki67 and DAPI. Stain compositions were plotted on a bar plot.
9) Inter-zonal comparison was performed by taking normalized signal from each zone and dividing by the largest value for each stain. Thusly, the zone with the highest value for a particular stain would have a value of 1. Quantitative results were displayed on a radial plot broken into two different panels.
10) Results of 8 and 9 analyzed to generate groupings of similar features.

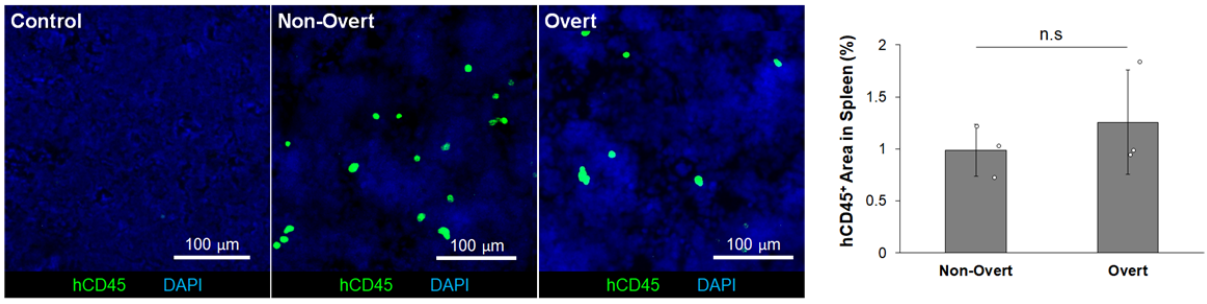

Fig. S19. Human PBMCs enter circulation in secondary mouse host. Spleens taken from non-injected (control) and hPBMC-injected mice. Non-overt spleens taken from mice without overt-metastasis bearing scaffolds. Overt spleen taken from mice with a scaffold with an overt metastasis. (n = 2, spleen retrieved from non-overt and overt metastatic tumor bearing mice) Data are mean ± s.d. Not significant, $P > 0.05$ via two-sided student t-test.

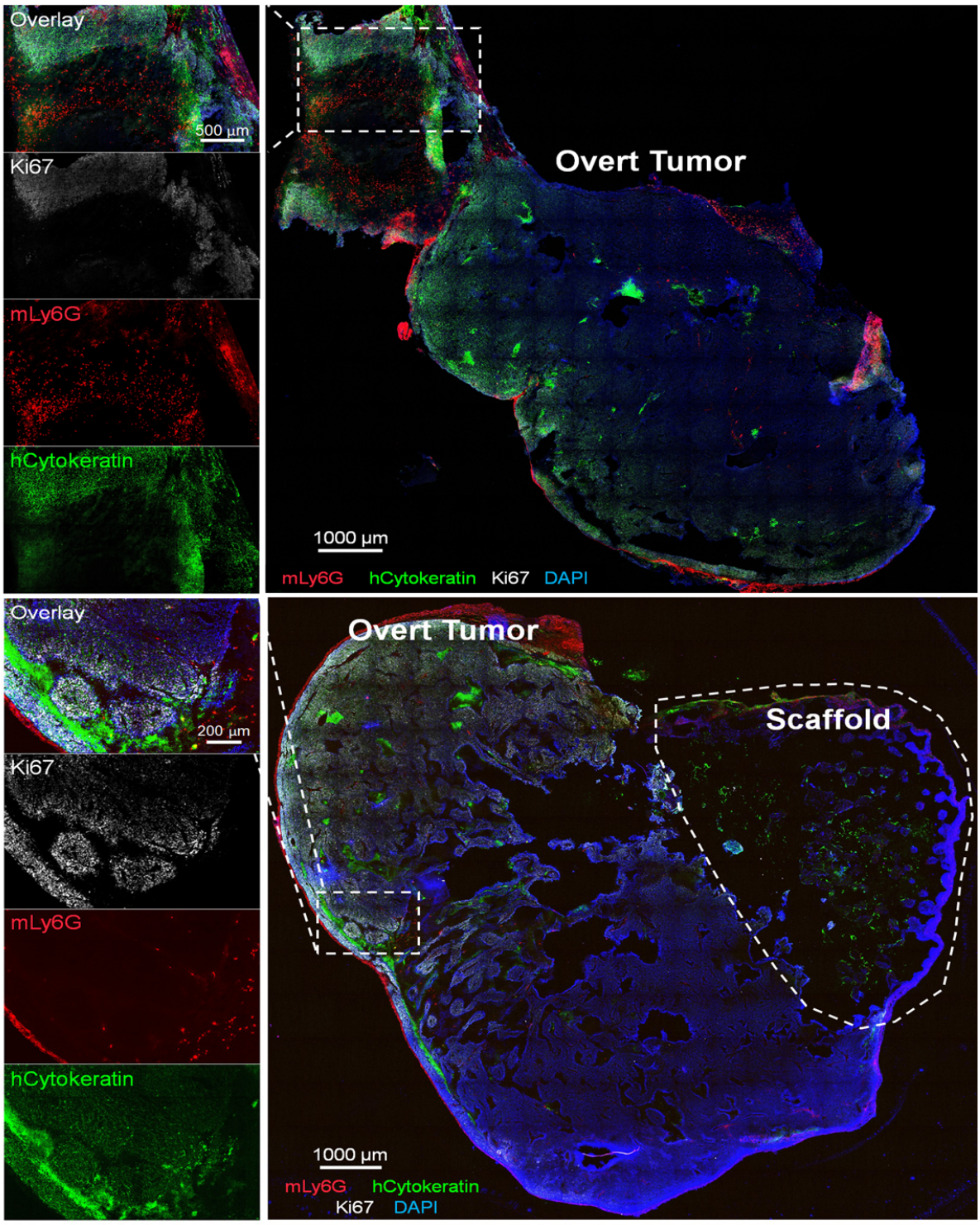

Fig. S20. IHS of mLy6G, Ki67 and hCytokeratin in independent overt metastasis. IHS of Ki67 and mLy6G localization in independent actively growing overt tumors beyond the boundaries of the scaffold. The identified feature was reproducibly observed in 3 independently characterized scaffolds including the one showed in Fig S17.

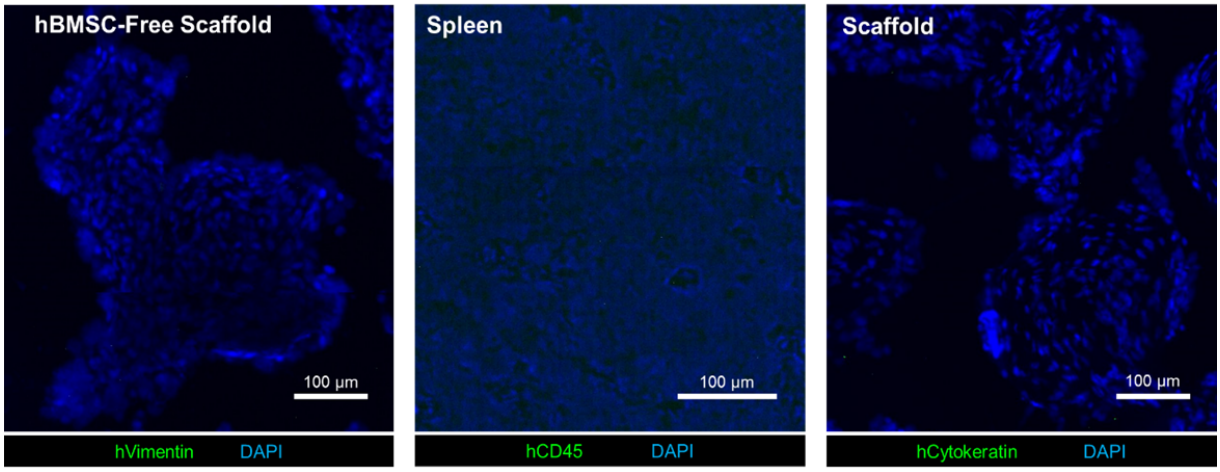

Fig. S21. IHS of hVimentin, hC45, and hCytokeratin against relevant mouse tissue to rule out cross-reactivity. This validation of antibody cross-reactivity was conducted one time.

Table S1. Antibody reagents.

PRIMARY ANTIBODIES			
Vendor	**Catalog Number**	**Chemical Name**	**Target**
DAKO	M072529-2	Mouse - Anti Human Vimentin	hStroma/hTumor
Abcam	ab5694	Rabbit - Anti Alpha Smooth Muscle Actin	Blood Vessel (CLARITY)
BD Pharmingen	550274	Rat - Anti Mouse CD31	Blood Vessel
BD Pharmingen	555480	Mouse - Anti Human CD45	hImmune
BD Pharmingen	555631	Mouse - Anti Human CD8	hCD8
BD Pharmingen	555344	Mouse - Anti Human CD4	hCD4
Abcam	ab16667	Rabbit - Anti Ki67	Proliferation
Abcam	ab107115	Chicken - Anti Human Cytokeratin 8	hTumor
BD Pharmingen	565409	Rat - anti mouse F4/80	mMacrophage
BD Pharmingen	557445	Rat - anti mouse Ly-6G Ly-6C	mNeutrophil
Lifespan Biosience	LS-C193787-100	Guinea Pig - Anti Human Cytokeratin	hTumor
BD Pharmingen	550392	Mouse - Anti Human CD44	hStem Cell
Abcam	ab15627	Rat - anti Mouse Ly6C	mMonocyte
ThermoFisher	PA513199	Rabbit - anti MMP	MMP-9

SECONDARY ANTIBODIES		
Vendor	**Catalog Number**	**Chemical Name**
Life Technology	A-11006	Goat anti-Rat IgG (H+L) Antibody - Alexa Fluor® 488
Life Technology	A-21424	Goat-Anti Mouse IgG (H+L) Antibody - Alexa Fluor® 555
Life Technology	A-11011	Goat Anti-Rabbit IgG (H+L) Antibody, Alexa Fluor® 568
Life Technology	A-21054	Goat-Anti Mouse IgG (H+L) Antibody - Alexa Fluor® 660
Life Technology	A-16058	Goat-Anti Chicken IgY (H+L) Antibody, biotin conjugate
Life Technology	Q10163MP	Qdot 705 Streptavidin Conjugate
Life Technology	A21449	Goat Anti-Chicken IgG (H+L) Antibody - Alexa Fluor® 647
Life Technology	A21450	Goat Anti-Guinea Pig IgG (H+L) Antibody - Alexa Fluor® 647
Life Technology	A10680	Goat Anti-Mouse IgG, IgM (H+L) Antibody - Alexa Fluor® 448

FACS		
Vendor	**Catalog Number**	**Chemical Name**
BD Bioscience	555483	Hu CD45 PE

ELISA		
Vendor	**Catalog Number**	**Chemical Name**
R&D Systems	DY206	Human IL-6 DuoSet
R&D Systems	DY217B	Human IL-10 DuoSet
R&D Systems	DY210-05	Human TNF-alpha DuoSet
R&D Systems	DY293B	Human VEGF DuoSet
R&D Systems	DY208	Human CXCL8/IL-8 DuoSet

Movie S1. Tissue cleared scaffold with blood vessel and tumor staining. This movie shows three-dimensional view of a single scaffold slice and follows vasculature and nearby DTCs throughout the scaffold.